Article

AMERICAN SCIENTIFIC PUBLISHERS

Journal of
Nanoscience and Nanotechnology
Vol. 18, 3954–3959, 2018
www.aspbs.com/jnn

New Route for Synthesis of Fluorescent SnO_2 Nanoparticles for Selective Sensing of Fe(III) in Aqueous Media

Gaurav Vyas, Anshu Kumar, Madhuri Bhatt, Shreya Bhatt, and Parimal Paul*

Analytical Division and Centralized Instrument Facility; Academy of Scientific and Innovative Research (AcSIR), CSIR-Central Salt and Marine Chemicals Research Institute, G. B. Marg, Bhavnagar 364002, India

A simple new route for synthesis of fluorescent SnO_2 and its application as an efficient sensing material for Fe^{3+} in aqueous media is reported. The fluorescent SnO_2 nanoparticles were obtained by oxidation of $SnCl_2$, which when used as reducing agent for the reduction of organic nitro compounds to corresponding amino compounds in ethanol. The SnO_2 nanoparticles have been characterized on the basis of powder-XRD, IR, UV-Vis, TEM, FESEM and EDX analysis and found that this material is highly fluorescent in aqueous media. Detail study revealed that this material functions as a selective probe for Fe^{3+} out of a large number of metal ions used. The oxygen vacancies (defects) generated on the surface of the SnO_2 during synthesis, are the source of emission due to recombination of electrons with the photo-excited hole in the valance bond. The quenching of emission intensity in presence of Fe^{3+} is due to the nonradiative recombination of electrons and holes at the surface. This material is used for estimation of Fe^{3+} in real samples such as drinking water, tap water and soil.

Keywords: Fe^{3+} Sensor, Fluorescent SnO_2, Sensing in Aqueous Media, Emission Lifetime.

1. INTRODUCTION

Commercially available SnO_2 is not fluorescent; however SnO_2 nanoparticles prepared by some special techniques such as discharge,[1] laser ablelation,[2,3] sol–gel,[4] hydrothermal reaction and microwave irradiation,[5] exhibit fluorescence and it has been used for different studies. Interestingly, we found that $SnCl_2 \cdot 2H_2O$ used for the reduction of various nitro compounds, viz. *p*-nitro toluene, 3-methyl-4-nitrophenol and tetranitro-calix[4]arene into their corresponding amino derivatives, produce SnO_2 nanoparticles (F-SnO_2), which are well dispersed in aqueous media and exhibit strong fluorescence. Thus a comparatively easy method has been developed for the preparation of fluorescent SnO_2. These SnO_2 nanoparticles have been characterized thoroughly and detail investigation on its sensing property towards metal ions revealed that it functions as a probe for selective sensing of Fe^{3+} in aqueous media.

Among transition metal ions, iron belongs to essential category and is associated with major metabolic pathways such as uptake and transport of oxygen to tissues during respiration.[6] Deficiency of iron affects the delivery of oxygen to cells resulting in fatigue, anaemia, poor work performance and low immunity.[7,8] On the other hand, its excess amount can catalyse the production of reactive oxygen species, which can damage biomolecules (lipids, nucleic acids and proteins).[9] Its toxicity is associated with disorders like Alzheimer's, Huntington's and Parkinson's disease.[10] Therefore, detection of Fe^{3+}, particularly in aqueous media, is highly desirable.

For the analysis of Fe(III), a number of instrument based analytical techniques are available. However, many of these methods are not simple and suitable for quick and onsite analysis, it also requires expensive instruments, tedious sample preparation procedures and sometimes detection limit is also a constraint. A few alternative methods have also been reported, among which colorimetric and fluorometric detection are most attractive.[11–13] In these methods of detection, mainly designed organic compounds have been used as chelate for selective binding of Fe^{3+} in various solvents and the sensing event is monitored optically by UV-Vis and fluorescence spectroscopy.[11–16] With recent development in nanotechnology, nanoparticles are emerging as important colorimetric and fluorometric

---

*Author to whom correspondence should be addressed.

1533-4880/2018/18/3954/006 doi:10.1166/jnn.2018.15025

receptor for various metal ions.[17–19] However, in the case of Fe^{3+}, nanoparticle based sensors are not common, recently there are some reports with quantum/carbon dots attached with some organic sensing moiety.[20–23] Examples of metal oxide based nanoparticles as sensing probe for Fe^{3+} is rarely reported.[24] Herein we report preparation and characterization of F-SnO_2 and its application for sensing of Fe^{3+} in aqueous media. To the best of our knowledge, no fluorescent SnO_2 nanoparticles have been reported so far for sensing of Fe^{3+}.

2. EXPERIMENTAL DETAILS

2.1. Materials and Methods

Infrared spectra were recorded on a Perkin-Elmer spectrum GX FT-system as KBr pellets. The UV/Vis and luminescence spectra were recorded on a CARY 500 Varian spectrophotometer and model Fluorolog Horiba Jobin Yvon spectrofluorimeter, respectively at room temperature.

The reagent stannous chloride of AR grade was purchased from SRL and used as such. The compounds 3-methyl-4-nitrophenol was purchased from Spectrochem and *p*-nitro toluene was purchased from SDFCL and used as such. The starting compounds *p-tert*-butylcalix[4]arene and calix[4]arene were synthesized as described in the literature.[25, 26]

2.2. Preparation of Fluorescent (F-SnO_2) Nanoparticles

F-SnO_2 nanoparticles were obtained during the synthesis of amino derivatives from the corresponding nitro compounds using $SnCl_2$ as a reducing agent. In a typical experiment nitro compounds (3-methyl-4-nitrophenol, *p*-nitro toluene and tetranitro-calix[4]arene) and $SnCl_2 \cdot 2H_2O$ were taken in ethanol and then glacial acetic acid (1 ml) was added as catalyst and the reaction mixture was heated under reflux for 24 h in dark (reaction vessel was covered by aluminium foil). After reflux, the hot solution was allowed to stand for 2–3 minutes for settling down some suspended large sized particles. The solution was then decanted separating the larger particles settled at the bottom and allowed to cool to room temperature. While cooling, corresponding amino compounds was precipitated, which was separated by filtration using sintered crucible (G-3), which allowed fine SnO_2 nanoparticles to pass through the filter bed. The solvent of the filtrate was then removed by rotary evaporation, the residue was washed three times with ethanol to remove trace amount of impurities if any, and then the mass was dispersed in water and stored for further use. The amino compounds were characterized and were used for some other purpose.

3. RESULTS AND DISCUSSION

3.1. Characterization of F-SnO_2 Nanoparticles

The reduction reaction (nitro to amino), which oxidized Sn^{2+} to Sn^{4+} and generated fluorescent SnO_2 is shown in Figure 1. The F-SnO_2 nanoparticles were isolated in solid state and were characterized on the basis of powder-XRD, IR, UV-Vis, SEM, TEM and EDX analysis. The powder-XRD pattern of the F-SnO_2 nanoparticles, recorded after drying the sample, is shown in Figure 2 (magenta colour) and that after calcination at 500 °C for 4 h is shown in red colour in the same figure. It may be noted that the peaks have not been changed after calcination suggesting that the compound is stable at 500 °C, up to which it is tested. The peaks in the diffractogram of the F-SnO_2 have been indexed to that of tetragonal SnO_2 (JCPDS no. 98-001-6635, P42/mnm, $a = b = 4.7360$ Å, $c = 3.1855$ Å). The diffraction peaks (110), (101) and (211) are clearly seen in the XRD profiles. The plane distance of, F-SnO_2 nanoparticles have an average lattice plane separation of 0.33 nm in the [110] direction and analysis of TEM image (discussed below) has also shown similar value.[27] The IR spectrum (Fig. 3) of F-SnO_2 exhibits strong peaks at 568 cm^{-1} and 668 cm^{-1}, which are assigned to Sn–O–Sn and Sn–OH for tetragonal cassiterite SnO_2.[28] The high resolution transmission electron microscopic (HRTEM) and scanning electron microscopic (SEM) images of F-SnO_2 nanoparticles are shown in Figure 4. The average size of the nanoparticles

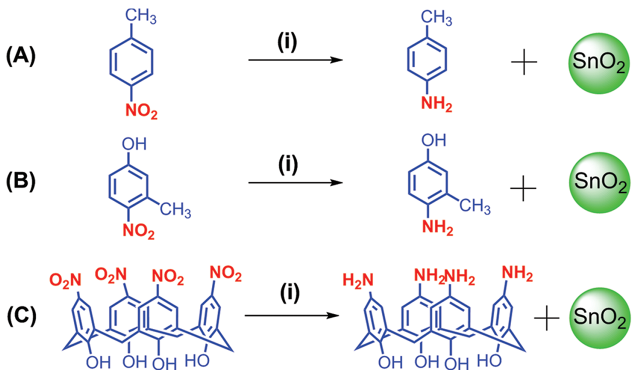

Figure 1. The reduction reaction (nitro to amino), which oxidized Sn^{2+} to Sn^{4+} and generated fluorescent SnO_2 is shown; (i) reaction condition is $SnCl_2 \cdot 2H_2O$, Glacial acetic acid (1 ml), Ethanol, 24 hrs, 90–100 °C.

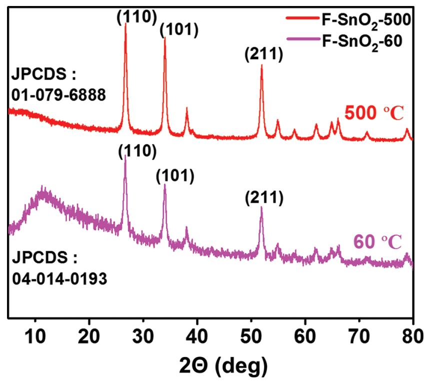

Figure 2. XRD profiles of the F-SnO_2 nanoparticles (Magenta colour) and the same after calcination at 500 °C (red) are shown.

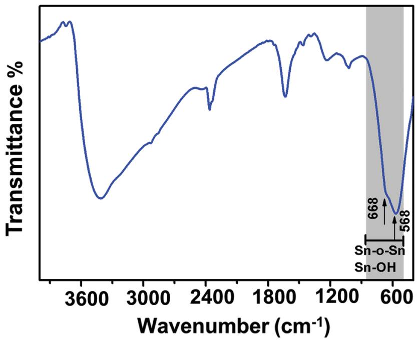

Figure 3. FT-IR spectrum of F-SnO_2 nanoparticles is shown.

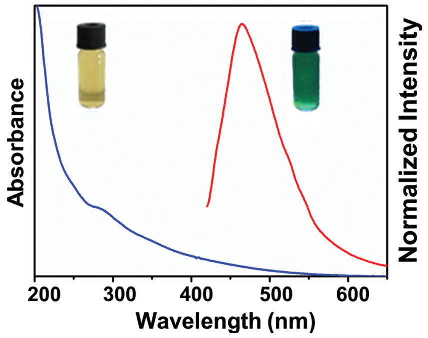

Figure 5. UV-vis (blue) and luminescence (red) spectra of F-SnO_2 dispersed in aqueous media with respective photographic images under UV light (inserted) are shown.

calculated from the HRTEM image (Fig. 4(a)) is found to be 3.0–5.0 nm. From the well-resolved lattice fringes (Fig. 4(b)), the calculated inter-planar distances is approximately 0.314 nm, which matched well with the (110) plane spacing of the tetragonal cassiterite SnO_2 structure and is consistent to the observation noted in the powder XRD data.[29, 30] The SEM image of F-SnO_2, shown in Figure 4(c), exhibits porous nature of the structure and the EDX analysis (Fig. 4(d)) confirmed the presence of tin. The UV-Vis and luminescence spectra of the aqueous dispersion of F-SnO_2 were recorded and shown in Figure 5. The absorption spectrum exhibits a weak shoulder around 300 nm and the luminescence spectrum exhibits a strong peak at 465 nm, which are consistent to the observations reported for other fluorescent SnO_2.[3, 15]

3.2. Application of F-SnO_2 as Sensor for Metal Ions

The sensing property of F-SnO_2 towards various metal ions was investigated by spectrofluorometric method. For this purpose, the emission spectra of F-SnO_2 in aqueous media were recorded with variation in concentration of the nanoparticles and also incubation time after addition of metal ions to optimise the experimental conditions Figure 6. From the experimental data, the optimum parameters found are 1 mg of F-SnO_2 in 1 mL water

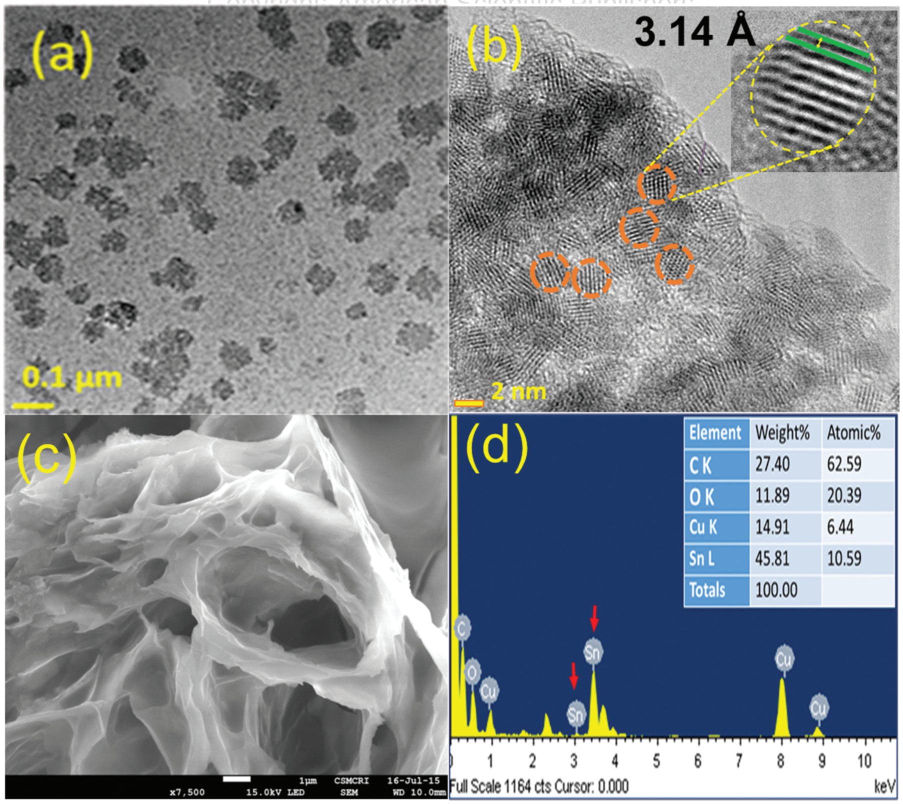

Element	Weight%	Atomic%
C K	27.40	62.59
O K	11.89	20.39
Cu K	14.91	6.44
Sn L	45.81	10.59
Totals	100.00	

Figure 4. (a) TEM image of F-SnO_2, (b) same image with high resolution showing lattice plane (inserted), (c) FESEM image of F-SnO_2 showing porous structure and (d) EDX data confirming the presence of tin are shown.

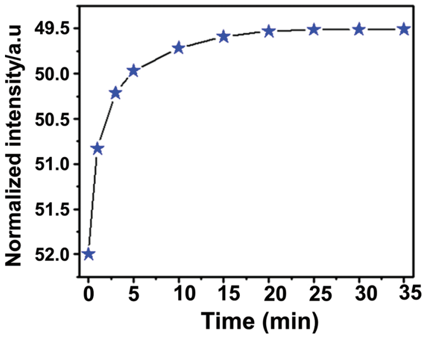

Figure 6. Plot of reaction time versus emission intensity after addition of Fe^{3+} is shown to optimise incubation time.

and 15 min incubation time. Subsequently all the experiments were carried out under this optimized condition. For the investigation of sensing property, the fluorescence spectra of F-SnO_2 dispersed in water was recorded and the same upon addition of the perchlorate salts of the metal ions such as Co^{2+}, Ni^{2+}, Cr^{3+}, Ba^{2+}, Cu^{2+}, Mg^{2+}, Li^{+}, Zn^{2+}, Cs^{+}, Ca^{2+}, K^{+}, Cd^{2+}, Pb^{2+}, Fe^{+2} and Fe^{3+} were recoded. The spectral changes are shown in Figure 7(a), the change in emission intensity at 465 nm (λ_{max} 400 nm) in the form of a bar diagram and the corresponding colour change under UV light is shown in Figure 7(b). It may be noted that except Fe^{3+} no other metal ions exhibited any spectral as well as colour change under UV light. To find out the concentration range, in which quenching of emission intensity is linear as a function of the concentration of metal ion added for its quantitative estimation, fluorescence titration was carried out with addition of increasing amount of Fe^{3+} (2 μM to 1000 μM). The spectral change and the plot of F_0/F versus concentration of Fe^{3+} (inset) are shown in Figure 8. It may be noted that with increasing the amount of Fe^{3+} added, the intensity of the emission band is decreased and the linearity is observed in the range 2 μM to 700 μM Figure 9, which suggests that amount of Fe^{3+} can be quantified if the concentration is within this range.

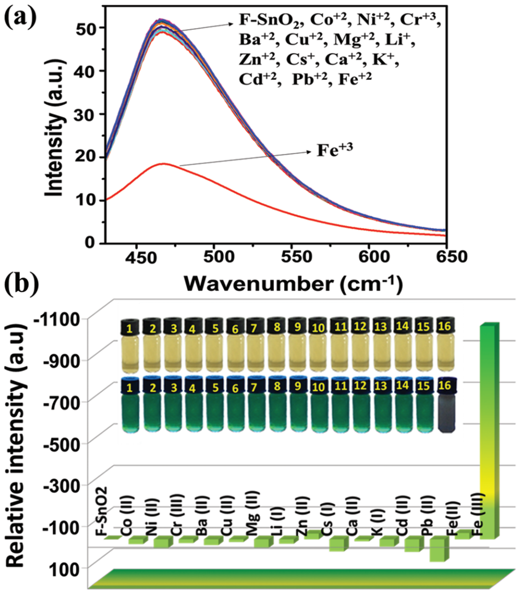

Figure 7. (a) Luminescence spectral change of F-SnO_2 (1 mg in 1000 μL) after addition of 15 different metal ions (1×10^{-3} M), (b) bar diagram showing the change in emission intensity at 465 nm (λ_{max} 400 nm) after addition of different metal ions and photograph showing no colour change under UV light for all metal ions, except Fe^{3+}, which exhibited a distinct colour change.

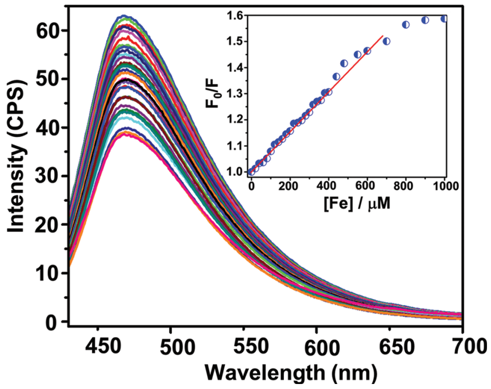

Figure 8. Luminescence spectral change for F-SnO_2 is shown upon addition of incremental amount of Fe^{3+} (2 μM to 1000 μM of 2×10^{-4} M). Inset: plot of F_0/F versus concentration of Fe^{3+} showing the linear relationship (2 μM to 700 μM).

3.3. Emission Life-Time

F-SnO_2 is a luminescent material and we were interested to investigate its emission life-time in absence and also in presence of Fe^{3+}. Figure 10 depicts the time resolved emission decay curve for F-SnO_2 dispersed in water, measured by the nanoLED-405 laser with excitation at 400 nm. The decay curve could be fitted into biexponential, analysis, which resulted in emission life-times of 0.99 ns and 6.62 ns. The fast decay component is due to the radiative recombination process and slow part is from the defect related emission.[5] The emission decay was again recorded upon addition of the perchlorate salt of Fe^{3+}, the analysis of the decay curve (Fig. 10) also fitted with biexponential pattern with life-times of 0.83 ns and 6.39 ns.

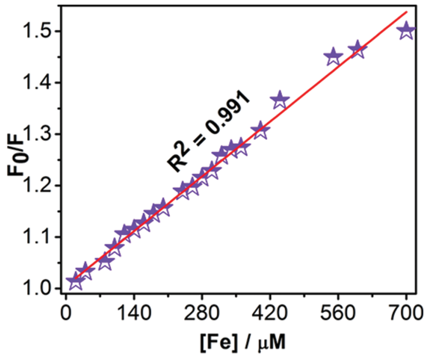

Figure 9. Plot of F_0/F luminescence spectral as a function of micromolar concentration of Fe^{3+} (2–700 μM) of F-SnO_2.

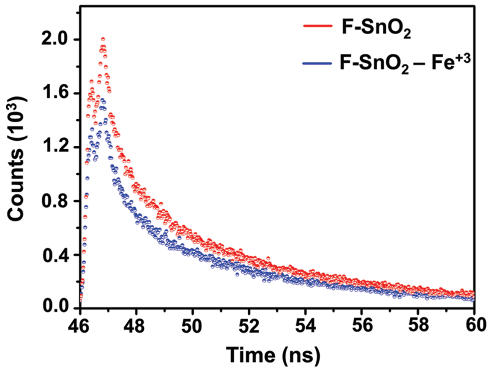

Figure 10. Emission decay of aqueous dispersion of F-SnO_2 in absence (red) and in presence of Fe^{+3} (blue) are shown.

Slight decrease in emission life-time of F-SnO_2 upon addition of Fe(III) with different concentrations, is consistent to the observation noted by others.[32]

3.4. Mechanism

As mentioned earlier, bulk SnO_2 is non-fluorescent, however some of the SnO_2 nanoparticles prepared by methods such as discharge,[1] laser ablelation,[2, 3] sol–gel,[4] hydrothermal and microwave irradiation[5] are fluorescent, which is due to defects generated during preparation.[33, 34] Oxygen vacancies in SnO_2 are known to be the most common defects and the origin of the emission can be assigned to the photo excited hole in the valance bond.[35, 36] After addition of Fe^{3+}, the quenching of emission intensity is associated with the nonradiative recombination of electrons and holes trapped at the surface of the particles.[37, 38] Apparently, ionic size and charge of the metal ions play a crucial role in the quenching process.

3.5. Application of the Method for Real Sample Analysis

F-SnO_2 is used for quantitative determination of Fe^{3+} in soil, drinking water and tap water. Drinking water (D) and tap water (T) samples were collected from this institute's campus and was tested for Fe^{3+} using F-SnO_2 with the aid of fluorescence measurement. The experiment did not show any change in fluorescence spectra, indicating the absence of detectable amount of Fe^{3+}, which is also confirmed by ICP analysis. Soil samples were collected from this institute as well as from out of the institute i.e., Rajkot, Gujarat. The test solution of the soil samples were prepared by the following procedure. 5 gm of soil was added into 100 mL of 0.5% H_2SO_4 and stirred for 2 hours at room temperature. Resultant solution was allowed to settle down and then decanted and centrifuged at 11000 rpm for 15 minutes and the supernatant solution was collected (S samples) for further analysis. The fluorescence spectra of F-SnO_2 upon addition of S samples (1 mL) were recorded. For quantitative determination of Fe^{3+} in the S samples, standard calibration curve (F_0/F vs. concentration plot) of Fe^{3+} was prepared from fluorescent spectral data of the aqueous F-SnO_2 containing known amount of Fe^{3+}. The amount of Fe^{3+} was further confirmed by ICP analysis (Table I). It may be noted that the ratio of the fluorescence intensity (F_0/F) was increased with increasing the concentration of Fe^{3+} and the data fit well on a straight line in the concentration range of 2 μM to 700 μM (Fig. 11). For drinking and tap water samples, measured amount of Fe^{3+} (Table I) was added into the drinking water (D) and tap water (T) and measured amount (1 mL) of these solutions were added into the aqueous dispersion of F-SnO_2 and the fluorescence spectra of these solutions were recorded. The amount of Fe^{3+} in these solutions were then determined by plotting the value of the ratio of fluorescence intensity (F_0/F) for each solution in the standard plot shown in Figure 11 and the corresponding values of the concentration of Fe^{3+} were determined, as shown in Figure 11. The amounts of Fe^{3+} estimated are compared with the amount added and the data for all the samples are shown in Table I and the results are satisfactory.

Table I. Experimentally obtained concentrations of Fe^{3+} and that in the spiked solutions functioned as unknown samples.

Samples	Found in samples by ICP (μM)	Spiked (μM)	By present method (μM)	Error (%)
[a]S1	180	–	177	1.6
[a]S2	230	–	240	4.3
[b]T1	–	95	83.8	11.8
[b]T2	–	390	388	0.5
[c]D1	–	170	163	4.1
[c]D2	–	470	507	7.8

Notes: [a]Soil, [b]tap water, [c]drinking water.

3.6. Comparison of the Method with Some Recent Reports

A comparison of the present study with that of some recent literature reports on sensing of Fe^{3+} using nanomaterials and quantum/carbon dots are summarized in Table II. It may be noted that the lower limit detection of the present study are comparable or better than many

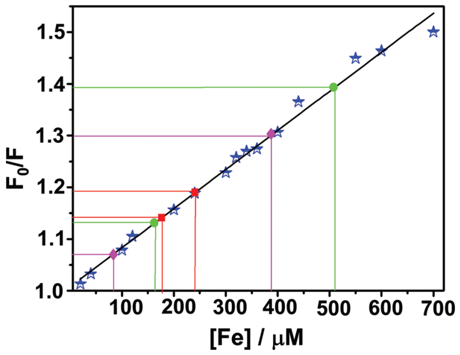

Figure 11. Linear plot generated by stock solution of Fe(III) in aqueous media. Values of the spike Fe(III) in drinking water (●) and tap water (■) and without spike in soil (♦) and the corresponding values of the concentration of Fe^{3+} found is shown in Table 1.

Table II. Comparison of various parameters of the present study with that of some other recent reports based on nanomaterials for sensing of Fe^{3+}.

Measure mode	Sensing nanomaterial	LOD (μM)	Medium	Ref.
Colorimetry/ Fluorimetry	RBD-UCNPs	1.2	Aqueous	[20]
Fluorimetry	Graphene Qdot's	10	Aqueous	[21]
Fluorimetry	TAZ-BTTC6 NPs	0.1	Aqueous	[22]
Colorimetry	pHEA-1/2/3 @AuNP40	8	Aqueous	[23]
Fluorimetry	AGO	–	Aqueous	[24]
Fluorimetry	F-SnO_2	2	Aqueous	This work

reported systems. The advantage of the present system is that the preparation of sensing material (F-SnO_2) is comparatively easy when a simple nitro compound such as *p*-nitro toluene is used for this purpose and also the corresponding amino compound thus obtained can be used for some other purpose. The F-SnO_2 obtained by this type of organic transformation is generally treats as waste material but the present study demonstrated that it is a very useful material for sensing of Fe^{3+} in aqueous media.

4. CONCLUSION

A simple method for the synthesis of fluorescent SnO_2 nanoparticles has been developed; otherwise it is difficult to prepare. The SnO_2 thus formed during the reduction of nitro compounds used to treat as waste material; however the present study demonstrated its application as a material for selective sensing of Fe^{3+} in aqueous media. Detail study revealed that the defect of oxygen vacancies on the surface of the F-SnO_2 generated during synthesis is the source of emission because of the recombination of electrons with the photo-excited hole in the valance band. After addition of Fe^{3+}, the quenching in emission intensity observed is due to the nonradiative recombination of electrons and holes at the surface of the nanoparticles. The F-SnO_2 thus obtained has also been used for analysis of Fe^{3+} in real samples and the results are satisfactory.

Acknowledgments: CSIR-CSMCRI publication No. 198. Financial support in the form of Network project (CSC 0134) from CSIR and fellowship from University Grant Commission (AK) are gratefully acknowledged. We thank G. R. Bhadu, Dr. D. N. Srivastava, J. C. Chaudhary, Laiya Riddhi P. and V. Vakani for recording TEM, SEM images, XRD data and IR spectra, respectively.

References and Notes

1. X. Liu, G. Zhou, S. W. Or, and Y. Sun, *RSC Adv.* 4, 51389 (**2014**).
2. J. Hu, Y. Bando, Q. Liu, and D. Golberg, *Adv. Funct. Mater.* 13, 493 (**2003**).
3. Z. W. Chen, J. K. L. Lai, and C. H. Shek, *Phys. Lett. A* 345, 391 (**2005**).
4. V. S. Anitha, S. S. Lekshmy, and K. Joy, *J. Alloys Compd.* 675, 331 (**2016**).
5. A. Kar, S. Kundu, and A. Patra, *J. Phys. Chem. C* 115, 118 (**2011**).
6. E. L. Que, D. W. Domaille, and C. J. Chang, *Chem. Rev.* 108, 1517 (**2008**).
7. A. Aroun, J. L. Zhong, R. M. Tyrrell, and C. Pourzand, *Photochem. Photobiol. Sci.* 11, 118 (**2012**).
8. S. Sen, S. Sarkar, B. Chattopadhyay, A. Moirangthem, A. Basu, K. Dhara, and P. Chattopadhyay, *Analyst* 137, 3335 (**2012**).
9. J. Xu, M. D. Knutson, C. S. Carter, and C. Leeuwenburgh, *PLoS One* 3, e2865 (**2008**).
10. V. Mahendran and J. Philip, *Langmuir* 29, 4252 (**2013**).
11. J. S. Kim and D. T. Quang, *Chem. Rev.* 107, 3780 (**2007**).
12. S. K. Sahoo, D. Sharma, R. K. Bera, G. Crisponi, and J. F. Callan, *Chem. Soc. Rev.* 41, 7195 (**2012**).
13. H. Zhou, J. Wang, Y. Chen, W. Xi, Z. Zheng, D. Xu, Y. Cao, G. Liu, W. Zhu, J. Wu, and Y. Tian, *Dye. Pigment.* 98, 1 (**2013**).
14. C. McDonagh, C. S. Burke, and B. D. MacCraith, *Chem. Rev.* 108, 400 (**2008**).
15. G. Zhang, B. Lu, Y. Wen, L. Lu, and J. Xu, *Sensors Actuators, B Chem.* 171, 786 (**2012**).
16. L. Qiu, C. Zhu, H. Chen, M. Hu, W. He, and Z. Guo, *Chem. Commun.* 50, 4631 (**2014**).
17. K. Saha, S. S. Agasti, C. Kim, X. Li, and V. M. Rotello, *Chem. Rev.* 112, 2739 (**2012**).
18. C.-C. Huang and H.-T. Chang, *Anal. Chem.* 78, 8332 (**2006**).
19. J. S. Lee, M. S. Han, and C. A. Mirkin, *Angew. Chemie-Int. Ed.* 46, 4093 (**2007**).
20. Y. Ding, H. Zhu, X. Zhang, J.-J. Zhu, and C. Burda, *Chem. Commun.* 49, 7797 (**2013**).
21. F. Xu, H. Shi, X. He, K. Wang, D. He, L. Yan, X. Ye, J. Tang, J. Shangguan, and L. Luo, *Analyst* 140, 3925 (**2015**).
22. J. Wang, X. Xu, L. Shi, and L. Li, *ACS Appl. Mater. Interfaces* 5, 3392 (**2013**).
23. D. J. Phillips, G.-L. Davies, and M. I. Gibson, *J. Mater. Chem. B* 3, 270 (**2015**).
24. L. He, J. Li, and J. H. Xin, *Biosens. Bioelectron.* 70, 69 (**2015**).
25. C. D. Gutsche and M. Iqbal, *Organic Syntheses* 68, 234 (**1990**).
26. C. D. Gutsche, J. A. Levine, and P. K. Sujeeth, *J. Org. Chem.* 50, 5802 (**1985**).
27. X. Xu, J. Zhuang, and X. Wang, *J. Am. Chem. Soc.* 130, 12527 (**2008**).
28. A.-H. Lim, H.-W. Shim, S.-D. Seo, G.-H. Lee, K.-S. Park, and D.-W. Kim, *Nanoscale* 4, 4694 (**2012**).
29. R. Liu, S. Yang, F. Wang, X. Lu, Z. Yang, and B. Ding, *ACS Appl. Mater. Interfaces* 4, 1537 (**2012**).
30. Z. Zhu, Y. Bai, X. Liu, C. C. Chueh, S. Yang, and A. K. Y. Jen, *Adv. Mater.* 28, 6478 (**2016**).
31. J. Xu, Y. Li, H. Huang, Y. Zhu, Z. Wang, Z. Xie, X. Wang, D. Chen, and G. Shen, *J. Mater. Chem.* 21, 19086 (**2011**).
32. P. J. Goutam, D. K. Singh, and P. K. Iyer, *J. Phys. Chem. C* 116, 8196 (**2012**).
33. Y. C. Her, J. Y. Wu, Y. R. Lin, and S. Y. Tsai, *Appl. Phys. Lett.* 89, 87 (**2006**).
34. X. T. Zhou, J. G. Zhou, M. W. Murphy, J. Y. P. Ko, F. Heigl, T. Regier, R. I. R. Blyth, and T. K. Sham, *J. Chem. Phys.* 128, 144703 (**2008**).
35. F. Gu, S. F. Wang, C. F. Song, M. K. Lü, Y. X. Qi, G. J. Zhou, D. Xu, and D. R. Yuan, *Chem. Phys. Lett.* 372, 451 (**2003**).
36. F. Gu, S. F. Wang, M. K. Lü, G. J. Zhou, D. Xu, and D. R. Yuan, *J. Phys. Chem. B* 108, 8119 (**2004**).
37. H. Zhang, Y. Chen, M. Liang, L. Xu, S. Qi, H. Chen, and X. Chen, *Anal. Chem.* 86, 9846 (**2014**).
38. M. Niu, F. Huang, L. Cui, P. Huang, Y. Yu, and Y. Wang, *ACS Nano* 4, 681 (**2010**).

Received: 9 March 2017. Accepted: 13 May 2017.